

GalactICS with Gas

N. Deg¹★, L. M. Widrow², T. Randriamampandry^{1,3}, and C. Carignan^{1,4}

¹*Department of Astronomy, University of Cape Town, Private Bag X3, Rondebosch 7701, South Africa*

²*Department of Physics, Engineering Physics, and Astronomy, Queen's University, Kingston, ON, K7L 3N6, Canada*

³*Kawli Institute for Astronomy and Astrophysics, Peking University, Beijing 100871, China*

⁴*Observatoire d'Astrophysique de l'Université de Ouagadougou (ODAUGO), BP 7021, Ouagadougou 03, Burkina Faso*

Accepted XXX. Received YYY; in original form ZZZ

ABSTRACT

We present a new version of the GALACTICS code that can generate self-consistent equilibrium galaxy models with a two-component stellar disc and a gas disc as well as a centrally-concentrated bulge and extended dark halo. The models can serve as initial conditions for simulations of isolated galaxies that include both hydrodynamics and collisionless dynamics. We test the code by evolving a pair of simple gas disc-halo models, which differ only in the initial temperature of the gas component. The models are similar to the ones considered in the Wang et al. except that here, the halo is live whereas they included the halo as a fixed potential. We find that the basic structural properties of the models, such as the rotation curve and surface density profiles, are well-preserved over 1.5 Gyr. We also construct a Milky Way model that includes thin and thick stellar disc components, a gas disc, a bulge, and a dark halo. Bar formation occurs in all disc-like components at about 1 Gyr. The bar is strongest in the thin disc while the gas disc contains the most prominent spiral features. The length of the bar in our model is comparable to what has been inferred for the Galactic bar.

Key words: galaxies: structure – galaxies: kinematics and dynamics

1 INTRODUCTION

A fundamental problem in galactic astronomy is the construction of self-consistent equilibrium models for individual galaxies. Such models can be used as a template for interpreting observations and inferring the gravitational potential of a galaxy and the structure of its dark halo (Widrow et al. 2008; Taranu et al. 2017). Furthermore, equilibrium models can provide initial conditions (ICs) for N-body simulations, which can in turn be used to study dynamical processes such as the formation of bars and spiral structure (Fux 1997; Athanassoula & Misiriotis 2002). Not only are these processes interesting in and of themselves, they also provide additional constraints on the models. For example, an equilibrium model that satisfies observational constraints but is nevertheless unstable to the formation of a strong bar is not a suitable model for a galaxy that has a weak bar or no bar at all (Sellwood 1985; Widrow et al. 2008; Randriamampandry et al. 2018).

It is invariably easier to model the evolution of collisionless matter (stars and dark matter) than gas. The dynamics of collisionless matter is determined solely by the gravitational field, which can be calculated efficiently using particle mesh or tree codes. On the other hand, the dynamics

of collisional matter depends on both the gravitational field and additional physics including hydrodynamical forces, star formation, feedback, and turbulence. Furthermore, many of these processes occur at scales below the resolution limit of simulations.

The complications associated with gas components extend to setting up ICs, especially, if one aims to follow a system from some equilibrium (but possibly unstable) state. ICs for collisionless systems in general require a self-consistent model for the phase space distribution function (DF) and the gravitational potential. Collisional systems also require models for the temperature of the gas as a function of position as well as the equation of state.

Springel et al. (2005) described a method for initializing a system with gas and stellar discs as well as a dark halo. The DF for the collisionless components are found by solving the Jeans equations (see (Hernquist 1993) and discussion below). For the gas disc, they assumed a simple equation of state $P = P(\rho)$. The vertical structure is then determined by solving the equations for hydrostatic equilibrium in the direction normal to the disc plane.

This method was refined Wang et al. (2010), who were particularly interested in initializing discs in their adaptive mesh refinement (AMR) simulations. In brief, they use an iterative approach to solve a set of equations describing the potential, surface density, and scale height of an isothermal,

★ E-mail: nathan.deg@ast.uct.ac.za

approximately exponential disc in the presence of an external potential. However, their simulations were limited to a gas disc in a fixed potential. In this paper we describe how to combine the GALACTICS (Galaxy Initial ConditionS) code (Kuijken & Dubinski 1995; Widrow, & Dubinski 2005; Widrow et al. 2008), which generates collisionless bulge-disc-halo systems, with the Wang et al. (2010) method of generating gas discs¹.

The problem of generating equilibrium ICs for collisionless systems, though more straightforward than that for collisional ones, is still a non-trivial task. The problem amounts to finding the DF for the collisionless components that satisfy (at least approximately) the coupled collisionless Boltzmann and Poisson equations. In the Hernquist method (Hernquist 1993), the velocity distribution of the stellar and dark matter components are assumed to be Gaussian with a dispersion found by solving the Jeans equations. Since solutions to the Jeans equations are not true solutions to the collisionless Boltzmann equation, these models typically relax to a state different from the one specified in the ICs (Kazantzidis et al. 2004). Other methods include MKGALAXY (McMillan & Dehnen 2007), which uses a guided relaxation algorithm, GALIC (Yurin & Springel 2014), whose algorithm has elements of the Schwarzschild method (Schwarzschild 1979) of building orbit libraries, and the iterative method presented in Rodionov et al. (2009); Rodionov & Athanassoula (2011).

In contrast with the Hernquist method, the GALACTICS DFs are based on the Jeans theorem, which states that functions of the integrals of motion are equilibrium solutions to the collisionless Boltzmann equation (CBE). In particular, the DFs for the bulge and halo are assumed to be functions of the energy, which are constructed to yield the target density profiles via the Eddington inversion formula Binney & Tremaine (2008). The DF for the disc is a function of the energy, angular momentum about the symmetry axis, and the vertical energy. Since the latter is only approximately conserved, the DFs are not exact solutions to the CBE. However, for thin discs, the approximation is excellent, and the model ICs for even thick discs are relatively stable. Armed with DFs in terms of the integrals of motion, GALACTICS solves the Poisson equation through an iterative algorithm, which meshes well with the Wang et al. (2010) prescription for building an equilibrium gas disc. The code has been used to study bar and spiral structure formation in the Milky Way (MW) (Widrow et al. 2008; Fujii et al. 2019), bending waves in discs (Chequers & Widrow 2017), how radial dispersions and the Galactic bar influence stellar populations (Debattista et al. 2017), merging dwarf galaxies (Lokas et al. 2014), and more.

Recently, a new method based on angle-action variables called AGAMA (Vasiliev 2019) has become available. It also involves an iterative scheme to solve Poisson’s equation with the additional step that for each iteration, one must construct that action variables in the new potential. One advantage of the method over GALACTICS is that it avoids the approximate “third integral”, E_z and therefore should be able to do a better job of modelling warm discs. On the other hand, the connection between angle-action variables

and the usual phase space coordinates of less transparent. Thus, it can be more difficult to build models with specific structural properties, such as a stellar disc with constant scale height (see, for example, (Chequers et al. 2018)). In principle, it should be straight forward to add a gas disc to an AGAMA model using a method similar to the one described in this paper.

Yet another approach can be found in Rodionov & Athanassoula (2011) who introduced an alternative iterative approach that allows one to build non-equilibrium galaxy models, such as discs embedded in triaxial halos. In their scheme, the system is evolved on a short time scale via the standard dynamical equations. Structure properties or parameters of the system, such as the surface density, are then reset and the system is again allowed to evolve. Ultimately, the sequence produces a system that is close to equilibrium.

The outline of the paper is as follows: In Section 2 we present the details of this new version of GALACTICS. We then examine two gas-halo models in Section 3. The models are similar to the ones considered in Wang et al. (2010) except in our simulations, the halo is ‘live’. In Section 4, we construct a 5-component MW model based on the best-fit model from McMillan (2017). We conclude with a discussion of our results in Section 5.

2 GALACTICS MODELS

The heart of GALACTICS is the construction of a DF for each of the components that together yield an axisymmetric model with the desired structural and kinematic properties. The total DF is given by

$$f(E, L_z, E_z) = f_b(E) + f_h(E) + f_{d,1}(E, L_z, E_z) + f_{d,2}(E, L_z, E_z) + f_g(E, L_z, E_z), \quad (2.1)$$

where E is the energy, L_z is the angular momentum about the symmetry axis of the system, and E_z is the energy of the vertical motions in the discs. For a time-independent and axisymmetric system, E and L_z are conserved while E_z is only approximately conserved for disc particles on nearly circular orbits.

The density ρ is determined by the integral of f over all velocities and since f is a function of E , which depends on Φ , Poisson’s equation is an implicit function of the Φ :

$$\nabla^2 \Phi = 4\pi \rho(R, z, \Phi) = 4\pi \int d^3 v f(E, L_z, E_z). \quad (2.2)$$

Note that here and throughout, we set Newton’s constant $G = 1$. GALACTICS numerically solves Eq. 2.2 using an iterative approach to obtain a self-consistent density-potential pair. First a target density profile is selected for each component. (The gas disc is treated somewhat differently. See Sec. 2.2). The corresponding potential is found by solving Poisson’s equation using an expansion in Legendre polynomials. The result is used, in turn, to calculate a new density and the process is repeated until the density-potential pair converges.

In detail, most of the algorithm is identical to that given in Widrow et al. (2008). By design, the bulge has a Sérsic density profile, the disc components are truncated exponential-sech² profiles, and the halo is a truncated double-power law. As with Widrow et al. (2008), the bulge

¹ The new version of GALACTICS is available upon request.

and halo use the Abel integral transformation (Binney & Tremaine 2008) to get their DF,

$$f_i(\epsilon) = \frac{1}{\sqrt{8\pi^2}} \int_E^0 \frac{d^2 \tilde{\rho}_i}{d\Phi^2} \frac{d\Phi}{\sqrt{\Phi - E}}, \quad (2.3)$$

where i is either the bulge or halo. In the presence of any of the disc components, this equation is solved using a spherical approximation of the disc potential for Φ_{tot} . It is important to note that this approximation is not used for the calculation of $\Phi(R, z)$ or $\rho(R, z)$, but is only used for Eq. 2.3. It is also worth noting that this method of evaluating Eq. 2.3 causes a degree of flattening, but the spheroid components remain isotropic and axisymmetric.

2.1 Stellar discs

The flattened nature of the stellar discs demands a different approach than the simple solutions used for the bulge and halo components. GALACTICS uses the DF presented in Kuijken & Dubinski (1995), which itself is based on Shu (1969) and Binney (1987).

The potential for this flattened system is calculated using a combination of spherical harmonics and an analytic 'fake' density-potential pair (Kuijken & Dubinski 1995). This pair, (ρ_{fd}, Φ_{fd}) , has the property that $\rho_d = \rho_{fd} + \rho_r$ and $\Phi_d = \Phi_{fd} + \Phi_r$ where ρ_r and Φ_r are residuals. The 'fake' components are designed to account for the higher order moments of the total potential, while the lower order moments are calculated by solving Poisson's equation for the residuals using a small number of l moments. The two are then summed together to give the total potential of the disc given some density. In practice, we find that $l_{max} = 10$ is sufficient for most models.

The GALACTICS DFs for the disc components are constructed to yield a vertical structure that is approximately isothermal. Thus, the vertical velocity dispersion is related to the thickness of the disc and the surface density. The DF is designed to yield a scale height that is approximately constant across the disc and a surface density that is approximately exponential with a scale radius R_d . Thus, the vertical dispersion profile is given by

$$\sigma_z^2 \simeq \sigma_{z,0}^2 e^{-R/R_d} \quad (2.4)$$

The radial dispersion profile appears as a free function in the disc DF. Here, we assume

$$\sigma_R^2(R) \simeq \sigma^2 e^{(-R/R_d)}. \quad (2.5)$$

This is based on the observations of Bottema (1993). The tangential dispersion is found through the epicycle approximation:

$$\sigma_\phi(R) \simeq \sigma_R(R) \frac{\kappa}{2\omega}, \quad (2.6)$$

where ω is the angular frequency and κ is the epicyclic frequency. Note that in the actual DF, σ_R , κ , and ω are written as functions of the guiding radius R_c , which is a function of L_z and hence an integral of motion. The approximations in the above equations reflect the fact that R_c is only approximately equal to R .

2.2 Gas disc

Wang et al. (2010) introduced two methods for generating isothermal equilibrium gas discs in a general galactic potential. We have adapted their 'potential' method. Since the disc is isothermal, the scale height increases as a function of the radius. We assume a target exponential surface density for gaseous component, which causes the space density in the midplane to be a decreasing function of radius.

Following Wang et al. (2010), we assume that the density of the gas disc is given by

$$\rho_g(R, z) = \rho_0(R) \exp\left(-\frac{\Phi_z(R, z)}{(\gamma - 1)\epsilon}\right), \quad (2.7)$$

where $\rho_0(R)$ is the mid-plane density, γ is the adiabatic index, ϵ is the specific internal energy, and $\Phi_z(R, z) = \Phi(R, z) - \Phi(R, 0)$. The specific internal energy depends on the temperature through the equation of state

$$\epsilon = \frac{1}{\gamma - 1} \frac{k_B T}{\mu m_p}, \quad (2.8)$$

where k_B is the Boltzmann constant, μ is the atomic weight of the gas, and m_p is the mass of the proton. For simplicity, that gas is assumed to be hydrogen and adiabatic so $\mu = 1$, $\gamma = 5/3$, and ϵ only depends on the gas temperature. It is convenient to re-parameterize the gas temperature as

$$c_0 = \frac{k_B T}{\mu m_p}, \quad (2.9)$$

which is similar to the specific internal energy and related to the sound speed. Combining the target exponential surface density,

$$\Sigma(R) = \Sigma_0 e^{-R/R_g} = \int_{-\infty}^{\infty} \rho_g(R, z) dz, \quad (2.10)$$

with $\rho_g(R, z)$ gives

$$\rho_0(R) = \frac{\Sigma_0 e^{-R/R_g}}{\int_{-\infty}^{\infty} e^{[-\Phi_z/c_0]} dz}. \quad (2.11)$$

The result is then included in Poisson's equation (Eq. 2.2). The algorithm for solving this equation proceeds as follows: First an initial surface density profile is used to estimate the gas disc potential. That potential is then used to calculate the scale height profile and total density, which are in turn used to get a new surface density and potential. The whole process is repeated until the system converges. Note that the surface density of the final system may deviate slightly from the target exponential surface density. As with the stellar disc, we use an analytic fake density-potential pair when solving Poisson's equation.

The gas disc density-potential pair is constructed at the same time as the total density-potential pair. The full GALACTICS algorithm for obtaining a self-consistent density potential pair is then given as follows:

- (i) Define the target profiles for all components.
- (ii) Estimate the total potential using Poisson's equation.
- (iii) Calculate new densities for the collisionless components using their DFs.
- (iv) Calculate the gas density using the current scale height profile and total potential.
- (v) Calculate new gas surface density and scale height profiles.

(vi) Repeat steps ii-v to achieve convergence.

We use a greatly simplified velocity structure for the gas disc compared to the stellar discs. The gas temperature is treated as a kinetic temperature that accounts for all turbulent motions. Therefore, the particles are initialized on purely rotational orbits where the speed is

$$V^2(R, z) = R \left. \frac{\partial \Phi}{\partial R} \right|_{z=0} + c_0 \left. \frac{\partial \ln \rho}{\partial \ln R} \right|_{z=0}, \quad (2.12)$$

with no random motions. Near the center it is possible for the gas pressure term to set $V^2 < 0$. While this condition has not occurred in any of the subsequent simulations, GALACTICS currently sets $V^2 = 0$ if the gas pressure term yields a negative result. In such cases we set $V^2 = 0$. An alternate method is to use the softening procedure outlined in [Hernquist \(1993\)](#). At this point we have not yet implemented and tested this in the context of GALACTICS. In addition, GALACTICS sets $v_z = 0$ for all gas particles as the vertical gravitational force is balanced against the gas pressure.

While this section has focused on the generation of a gas disc within the GALACTICS methodology, it is worth noting that this same algorithm can be included in the AGAMA method with little in the way of modifications since AGAMA also uses an iterative approach to calculate the total potential and density. However, since GALIC, and the Hernquist method do not include an iterative adjustment of the total potential, it would be difficult to modify those algorithms to utilize this particular method of constructing a gas disc. It would also be difficult to implement this method of gas disc construction into MKGALAXY due to differences in how the iterative calculation of the potential is performed. Nonetheless, gas discs could be generated in all these algorithms using alternate methods than the process utilized here.

3 GAS ONLY MODELS

In this section we describe testbed simulations that involve a gas disc and dark halo. The ICs roughly correspond to the Gas0 and Gas4 models of [Wang et al. \(2010\)](#). They have the same structural properties for the two components and differ only in the gas temperature. In particular, the dark halo has an NFW profile with scale length $r_h = 17.8$ kpc and velocity scale parameter (in GALACTICS parameterization) $\sigma_h = 389 \text{ km s}^{-1}$. This velocity scale parameter implies an NFW density parameter of $\rho_0 = \sigma_h^2 (2\pi r_h)^{-2} \simeq 1.77 \times 10^7 M_\odot \text{ kpc}^{-3}$. The gas disc has a mass of $M_d = 10^{10} M_\odot$ and an exponential scale length $R_g = 3.5$ kpc. The resultant rotation curve rises slowly to about 180 km s^{-1} at a radius of 30 kpc. The gas contribution to the rotational speed is always subdominant indicating that the disc will be stable to global perturbations. Following [Wang et al. \(2010\)](#) we set the gas temperature in the GalactICS-Gas0 model to $T = 4 \times 10^4$ K and the temperature in the GalactICS-Gas4 model to $T = 8 \times 10^3$ K. With these values, we expect the GalactICS-Gas0 model to be stable to local perturbations and the colder GalactICS-Gas4 model to be unstable (see Figure 4 of [Wang et al. \(2010\)](#)).

The DFs for the models are sampled with 1M gas particles and 5M halo particles and evolved for 1.6 Gyr using

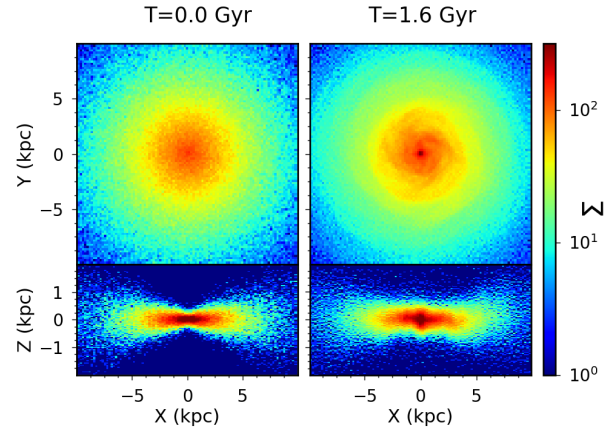


Figure 1. The surface density (upper panel) and cross-sectional density (lower panel) of the GalactICS-Gas0 model gas disc at $T = 0$ Gyr (left) and $T = 1.6$ Gyr (right). The units are M_\odot/pc^2 and M_\odot/pc^3 respectively.

the Gadget 2 N-body code ([Springel 2005](#)). We use an adaptive softening length with an initial length set to 0.005 kpc and a maximal softening lengths of 0.5 kpc. This is smaller than the recommended softening lengths from [Rodionov & Sotnikova \(2005\)](#). However, the gas discs for both models are quite thin in the central kpc. As such, we feel that this small scale length is justified. In the simulation, we use an adaptive time step with a maximal step of 0.01 Gyr (which also matches the snapshot frequency). The Courant factor in the GADGET 2 simulation is set equal to 0.25.

We stress that in our simulations, the halo is ‘live’ whereas the halo in the [Wang et al. \(2010\)](#) simulations is treated as a static halo potential. Moreover, [Wang et al. \(2010\)](#) ran their simulations with the adaptive-mesh-refinement code RAMSES ([Teyssier 2002](#)) whereas GADGET 2 models the gas using smooth particle hydrodynamics.

3.1 The GalactICS-Gas0 model

Figure 1 shows the initial and final surface and cross-sectional densities for the GalactICS-Gas0 model. It is clear that there has been some evolution of the system. In particular, the central surface density of the disc has increased (upper panels), as has its scale height (lower panels).

The changes in the gas surface density and thickness are highlighted in Figs. 2 and 3 respectively. In Fig. 2 we see that the surface density has increased significantly in the central regions. In addition, the sharp cut-off at the edge of the disc has been smoothed out. On the other hand, at intermediate radii ($1 < R < 15$ kpc), the evolved surface density is consistent with the initial one. The disc thickness increases at all radii, with the largest increase occurring in the central 0.5 kpc.

Further clues as to the evolution of the system can be found in Fig. 4, which shows that the azimuthally averaged rotation curve (calculated from the gravitational potential) as well as a scatter plot of gas particle azimuthal velocities. Although the gas disc is initialized with purely rotational motions, it is clear from the figure that the gas particles gain random azimuthal (and presumably radial and verti-

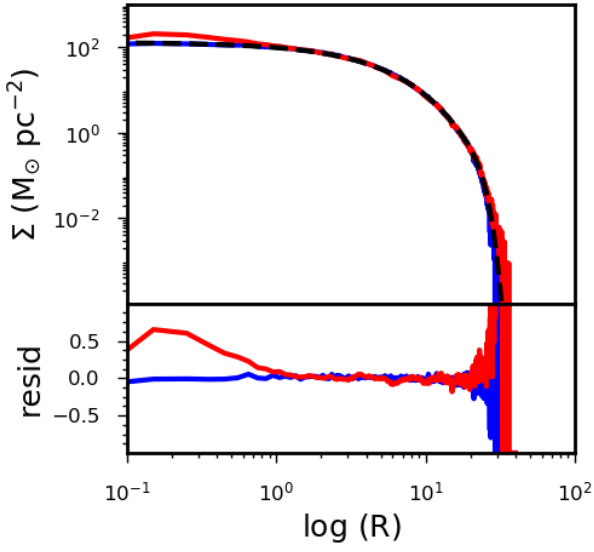


Figure 2. The azimuthally averaged surface density of the GalactICS-Gas0 gas disc as a function of radius (top) and the density residuals (bottom). The dashed black curve is the initial analytic profile and the solid blue and red lines are the surface densities at $T = 0$ and 1.6 Gyr respectively. The distance units are kpc.

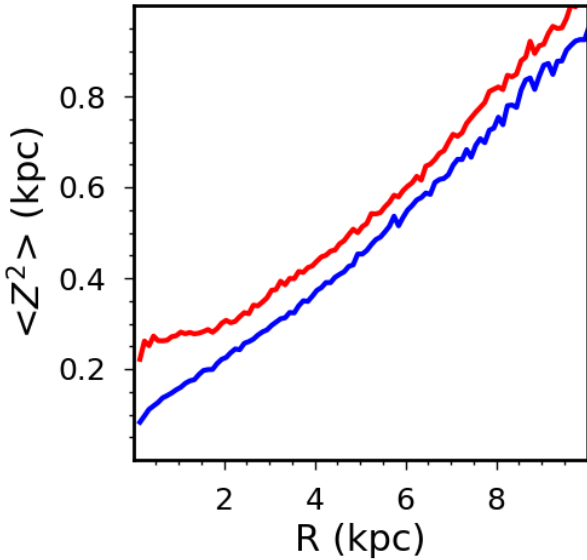


Figure 3. The average gas disc thickness of the GalactICS-Gas0 model as a function of radius for $T = 0$ Gyr (blue) and $T = 1.6$ Gyr (red).

cal) motions. These random motions represent a transfer of rotational energy to the random kinetic energy of the gas particles. It is therefore not surprising that the disc “puffs up” a bit and also compresses slightly in the radial direction, thereby increasing the central surface density. Note that the gravitational rotation curve stays very nearly constant over the duration of the simulation.

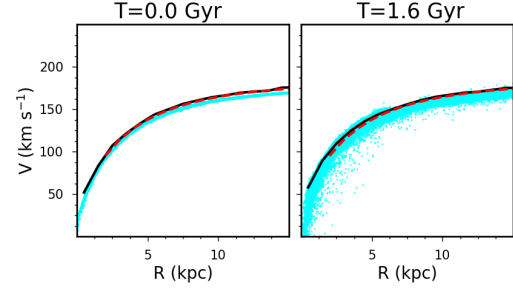


Figure 4. The rotation curve of the GalactICS-Gas0 model at $T = 0$ (left) and 1.6 (right) Gyr. The dashed red curve is the initial analytic velocities, the solid black line is the expected velocity from the azimuthally averaged radial force, the cyan points at the tangential velocities of particles.

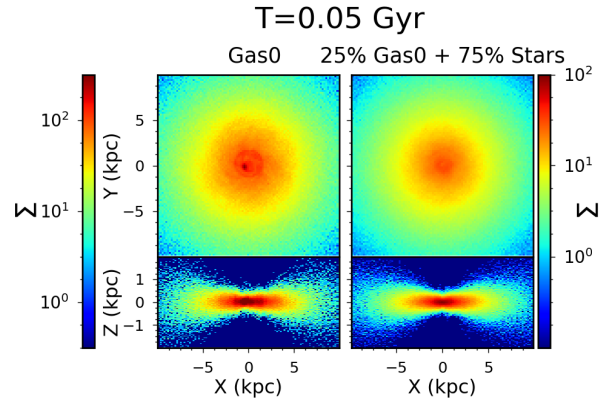


Figure 5. The surface density (upper panels) and cross-sectional density (lower panels) of the gas disc for the GalactICS-Gas0 model and Quarter-Gas0 model at $T = 0.05$ Gyr. The differing scales for the left and right panels is to highlight the over-density transient present in the Gas0 model. The units of surface density and cross-sectional density are M_{\odot}/pc^2 M_{\odot}/pc^3 respectively.

To investigate the transients in this simulation we show, in Fig. 5, the face-on and edge-on projections of the density after just 50 Myr. A ring of particles corresponding to a axisymmetric density wave, is clearly visible.

Apart from the scattering of disc particles, a second possible cause of the transients may be in the use of the ‘fake’ gas disc density-potential pair. The gas disc is extremely thin near its centre with a scale height of less than 100 pc. Moreover, the thickness changes rapidly with radius there. Thus, it may be difficult for our fake-disc/Legendre polynomial expansion scheme to full capture the potential. Small errors in the potential solver can lead to an incorrect scale height and an over/under pressure, thereby causing a transient wave, as is seen in Fig. 5.

To be clear the approximation that causes the transient only fails in regions where the value of Φ_z is dominated by the gas disc contribution. At moderate radii the halo dominates Φ_z and the small errors from the gas potential approximation are inconsequential. To illustrate this point, we generated a Gas0-stars model where the gas disc is replaced by a two-component disc of gas and stars with a mass ra-

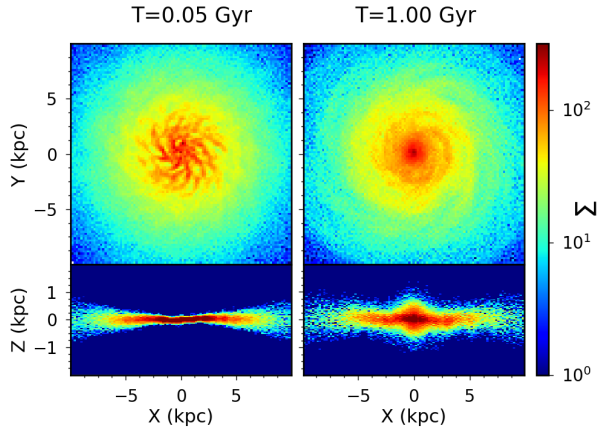


Figure 6. The surface density (top) and cross-sectional density (bottom) of the GalactICS-Gas4 gas disc at $T = 0.05$ and $T = 1.00$ Gyr. The surface density and cross-sectional density units are M_{\odot}/pc^2 M_{\odot}/pc^3 respectively.

tio of 1 : 3. The velocity dispersion for the stars is assumed to be exponential dispersion as in Eq. 2.10 with a central dispersion of $\sigma_{r,0} = 100 \text{ km s}^{-1}$. The right panel of Fig. 5 shows the gas disc of this system at 50 Myr. In contrast with the GalactICS-Gas0 model, there is no transient wave even though the system has the same surface density profile. It is worth noting that the thickness of the stellar disc also thickens the gas disc in the central regions while decreasing the degree of flaring in the outer regions.

3.2 The GalactICS-Gas4 Model

We next consider the GalactICS-Gas4 model, which is unstable to local perturbations. In the Wang et al. (2010) realization of this model, the gas disc rapidly fragments (see the lower left panel of their Figure 5). Our realization of this model is also unstable, but it evolves slightly differently.

Fig. 6 shows our gas disc at 50 Myr and 1 Gyr. The initially very thin disc thickens significantly by 1 Gyr. At 50 Myr, the disc has begun fragmenting into a strong spiral structure. This fragmentation is less symmetric than that seen in the Wang et al. (2010) model due to both the random sampling procedure of GALACTICS and the live halo. By 1 Gyr this instability has evolved in such a way to produce thick central region with poorly defined spiral arms.

Figure 7 shows the initial disc thickness and the thickness at $T = 1.0$ Gyr. Comparing this to Fig. 3 it is clear that the Gas4 gas disc is initially about half the thickness of the GalactICS-Gas0 disc. The height in the central region increases to about the same as the Gas0 model in the final timesteps, but rather than staying at some constant thickness before flaring in the outer radii, the Gas4 thickness decreases to a minimum near 3 kpc before flaring to the outer radii.

Figure 8 shows the evolution of the azimuthally averaged surface density profile. The changes to the averaged profile are similar in scale and origin to the changes that occur for the GalactICS-Gas0 model.

It is important to note that both the GalactICS-Ga0

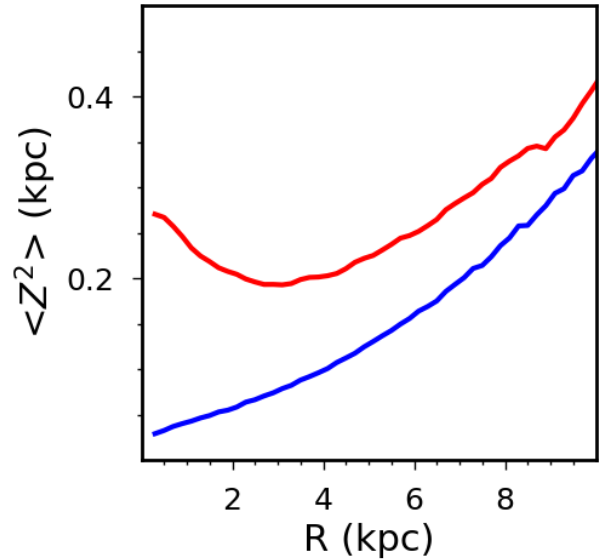


Figure 7. The average gas disc thickness of the GalactICS-Gas04 model as a function of radius for $T = 0$ Gyr (blue) and $T = 1.0$ Gyr (red).

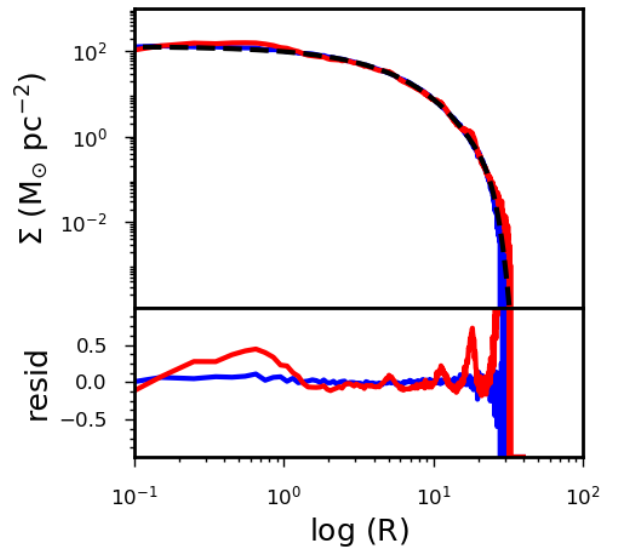


Figure 8. The azimuthally averaged surface density of the GalactICS-Gas4 gas disc as a function of radius (top) and the density residuals (bottom). The dashed black curve is the initial analytic profile and the solid blue and red lines are the surface densities at $T = 0$ and 1.0 Gyr respectively. The distance units are kpc.

and Gas4 models are fairly different from real galaxies. Nonetheless, these two models demonstrate the ability of GALACTICS to generate both stable and unstable models. These models are relatively straightforward, consisting of only a halo and a thin (or very thin) gas disc.

4 A MILKY WAY MODEL

In this section, we demonstrate the utility of our new GALACTICS code by generating and evolving a realistic five-component model for a MW-like galaxy. Our model is based on the mass models from [McMillan \(2017\)](#). In that paper observations of Maser line-of-sight velocities, the proper motion of Sgr A*, the terminal velocity curve, the local vertical force, and the total mass within 50 kpc were used to constrain the parameters of an analytic model for the mass and gravitational potential of the Milky Way. The [McMillan \(2017\)](#) model comprised an NFW halo, thin and thick stellar discs, a bulge based on [Bissantz & Gerhard \(2002\)](#), and both a HI and H₂ gas discs.

In this paper, we build a GALACTICS model that uses the “most likely” parameters from [McMillan \(2017\)](#). We assume an NFW halo with $\sigma_h = 298 \text{ km s}^{-1}$ and $r_h = 19.6 \text{ kpc}$ ($\rho_0 = 8.55 \times 10^6 M_\odot \text{ kpc}^{-3}$). For the thin disc we assume $M_{d,\text{thin}} = 3.52 \times 10^{10} M_\odot$, $R_{d,\text{thin}} = 2.5 \text{ kpc}$ and $z_{d,\text{thin}} = 0.28 \text{ kpc}$ while for the thick disc we assume $M_{d,\text{thick}} = 7.2 \times 10^9 M_\odot$, $R_{d,\text{thick}} = 3.02 \text{ kpc}$, $z_{d,\text{thick}} = 0.83 \text{ kpc}$. Note that the scale height parameters are somewhat smaller than those used in [McMillan \(2017\)](#) to account the fact that the vertical structure in those models is exponential in $|z|$ whereas GALACTICS discs have an approximately $\text{sech}(z)^2$ form. The latter form naturally arises from the assumption that the discs are vertically isothermal.

By design GALACTICS bulges have a surface density profile that is given, to a good approximation by the Sérsic profile. To convert the [Bissantz & Gerhard \(2002\)](#) bulge from [McMillan \(2017\)](#) to a Sérsic one we performed a simple parameter search using the inner 2 kpc of the density profile. This search yielded $n \approx 2$ for the Sérsic index, $R_b \approx 0.64 \text{ kpc}$ for the radial scale length, and $\sigma_b = 304 \text{ km s}^{-1}$ for the velocity scale (see [Widrow et al. \(2008\)](#)).

Finally, we consider the gas components from [McMillan \(2017\)](#). Since our current version of GALACTICS has just a single exponential gas disc we fit this model to the total gas surface density from the combined HI and H₂ gas discs of [McMillan \(2017\)](#). Fig. 9 shows the comparison of the GALACTICS disc to the two discs in [McMillan \(2017\)](#). Our disc has $M_g = 2.39 \times 10^{10} M_\odot$ and $R_g = 13.1 \text{ kpc}$. Note that the [McMillan \(2017\)](#) discs have a hole in the centre so the structure of the gas components in the two models is rather different though the total mass in gas is very similar. Our model is constructed with a gas temperature of 10^4 K .

As with the models in the previous section, the system is evolved using GADGET-2. Our N-body model comprises 10^6 gas particles, 5×10^5 bulge particles, 2×10^6 thin disc particles, 10^6 thick disc particles, and 5×10^6 halo particles. The system is evolved for a total of 2 Gyr.

Fig. 10 shows circular speed decomposition of our model at $T = 0$ and $T = 1 \text{ Gyr}$. We see that the disc components (primarily the thin disc) dominate the radial force at radii of about two disc scale lengths. Thus, we expect the model to form a bar and spiral structure, which indeed it does. The surface density profiles of the different components are shown in Fig. 11. The thin disc dominates the baryon mass budget at radii $R < 13 \text{ kpc}$ except in the innermost region where the bulge makes a comparable contribution to the surface density. On the other hand, the gas disc, which in

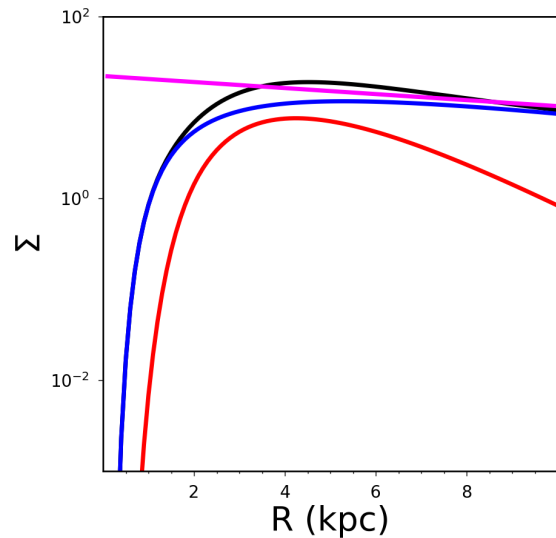


Figure 9. The two holed gas discs found by [McMillan \(2017\)](#) compared to our best fitting exponential gas disc (magenta). The blue and red curves are the HI and H₂ gas discs and the black curve is the total gas surface density. The surface density is in units of $M_\odot \text{ pc}^{-2}$.

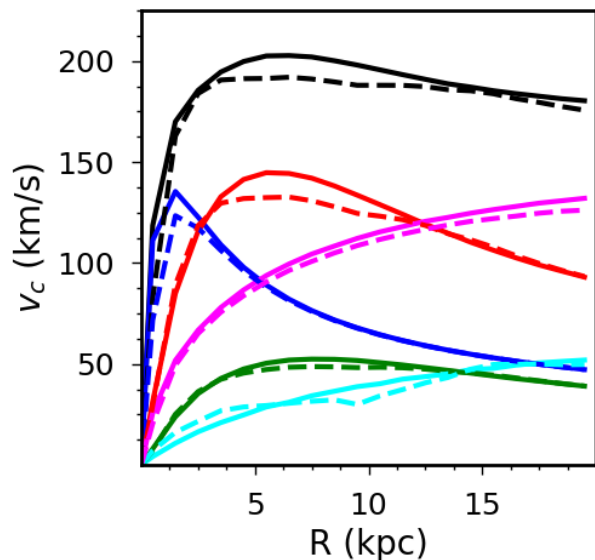


Figure 10. The rotation curve of our MW model at $T = 0$ (solid lines) and $T = 1 \text{ Gyr}$ (dashed lines). The black, blue, red, green, cyan, and magenta lines are the total curve and the contribution of bulge, thin disc, thick disc, gas disc, and halo respectively.

this model has a larger radial scale length, dominates the outer disc.

The evolution of the circular speed and azimuthally averaged surface density profiles is due to the formation of a bar and spiral arms. From the surface density profiles we see that mass in the disc components moves outward from

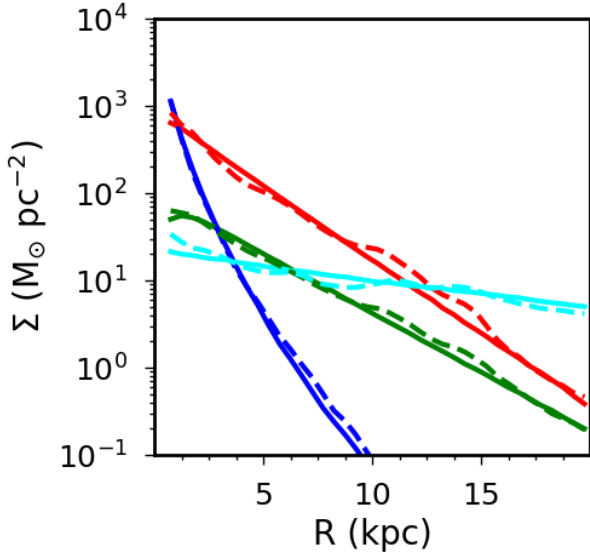


Figure 11. The surface density profiles of the four MW baryonic components at $T = 0$ (solid lines) and $T = 1$ Gyr (dashed lines). The bulge, thin disc, thick disc, and gas disc are the blue, red, green, and cyan lines respectively.

$R \sim 3 - 5$ kpc to $R \sim 9 - 11$ kpc. This mass redistribution leads to a change in the shape of the rotation curve.

Figure 12 shows a snapshot of the model at $T = 1$ Gyr. As noted above, the disc components have all developed bar and spiral structure, although the bar strength varies considerably between the various disc components. The difference between the components can be seen more clearly in Fig. 13, which shows the evolution of A_2 for the three disc components as a function of radius and time where A_2 is the amplitude of the $m = 2$ Fourier component for the surface density where m is the usual azimuthal mode number. At all times and radii, the thin and thick discs show similar structure, although the A_2 moment is always weaker in the thick disc. Both stellar discs show a clear bar component with peaks in the A_2 moment at $R \approx 2.5$ kpc for $T \geq 1.0$ Gyr. The gas disc has a much more transitory structure. While there is some structure in the bar region, the dominant $m = 2$ structures are at larger radii and clearly correspond to the two-armed spiral structure seen in Fig. 12.

The difference in the bar strengths between the thin and thick discs is similar what is observed in both nature and simulations. Athanassoula (1983) ran simulations of galaxies with single discs and noted that dynamically colder discs formed thinner bars than hotter discs. Athanassoula (2003) followed this investigation with a theoretical and numerical exploration of the relationship between angular momentum transfer and bar properties. In that work it was found that increased disc velocity dispersions inside the co-rotation radius decreased the bar strength. More recently Athanassoula et al. (2016) ran simulations of merging galaxies. They found that the thin disc also formed a stronger bar component than the thick disc. The bar present in their thick discs have the same length and orientation as in the thin disc bar, but have larger vertical extents and are significantly more oval in nature. Athanassoula (2018) found similar results using a more

advanced analysis of these merging simulations clearly show the difference between the thin and thick discs. The simulations of Bekki & Tsujimoto (2011) examined the formation of the bulge from a single or two-disc scenario. They found that a thick disc is less influenced by the presence of a bar, allowing for a steep vertical metallicity gradient. Similarly, Debattista et al. (2017) utilized variety of different simulations to show that populations with lower radial velocity dispersions form stronger bars than those that are dynamically hotter. Fragkoudi et al. (2017) found similar results in their simulations, noting that the thin disc bar was $\sim 50\%$ stronger than the bars found in the thick disc, as well as being significantly more elongated.

The bar and spiral structure seen in our evolved model are similar to what are observed in the Milky Way. For example, the bar in the MW has a length of about 3–4 kpc (see Bissantz & Gerhard (2002) and references therein), which is comparable to what we find in our simulation. Likewise, the spiral structure shows a strong two-armed pattern with evidence for weaker four or more armed spiral structure. Our structures do seem to have a tighter winding pattern than what is seen in the Galaxy.

The origin of the bar and spiral structure pattern of the Milky Way is still an open question. For example, Purcell et al. (2011) argued that these structures might be the result of an encounter between the disc and the Sagittarius dwarf. Our results suggest that the disc can form structures of this type through internal instabilities. However, this simulation has only been run for a few orbits. Further investigation must be done to examine whether the bar and spiral structure seen here will persist over dozens of dynamical times.

5 SUMMARY AND CONCLUSIONS

In this paper, we have introduced a new version of the GALACTICS code that is able to generate equilibrium models for a galaxy consisting of thin and thick stellar discs, a stellar bulge, a dark halo, and gas disc. The models can be used to generate ICs for N-body simulations that, in turn, can be used to study the dynamics of real galaxies and, in particular, the formation of bars and spiral structure.

Test bed simulations of models with just a gas and dark halo showed the ability of GalactICS to produce both stable and unstable models. A transient is present in some gas-halo only models. The inclusion of a stellar disc suppresses these transients, yielding stable models. Regardless of the presence of a transient, the azimuthally averaged surface densities remain roughly constant. The tangential velocities of the gas particles have an increase in random motions, but the gravitationally calculated circular speed remains constant.

We demonstrated the applicability of the model by constructing a multi-component *dynamical model* for a MW-like galaxy based on the *mass model* of McMillan (2017). We found that this model produces a relatively strong bar and spiral structure by $T = 1.0$ Gyr. The bar is present in all of the disc-like baryonic components though strongest in the thin disc. Spiral arms are also present in all of the disc components though noticeably thinner and more prominent in the gas disc.

GALACTICS provides an excellent tool for dynamical studies of galaxies. In particular, it generates N-body

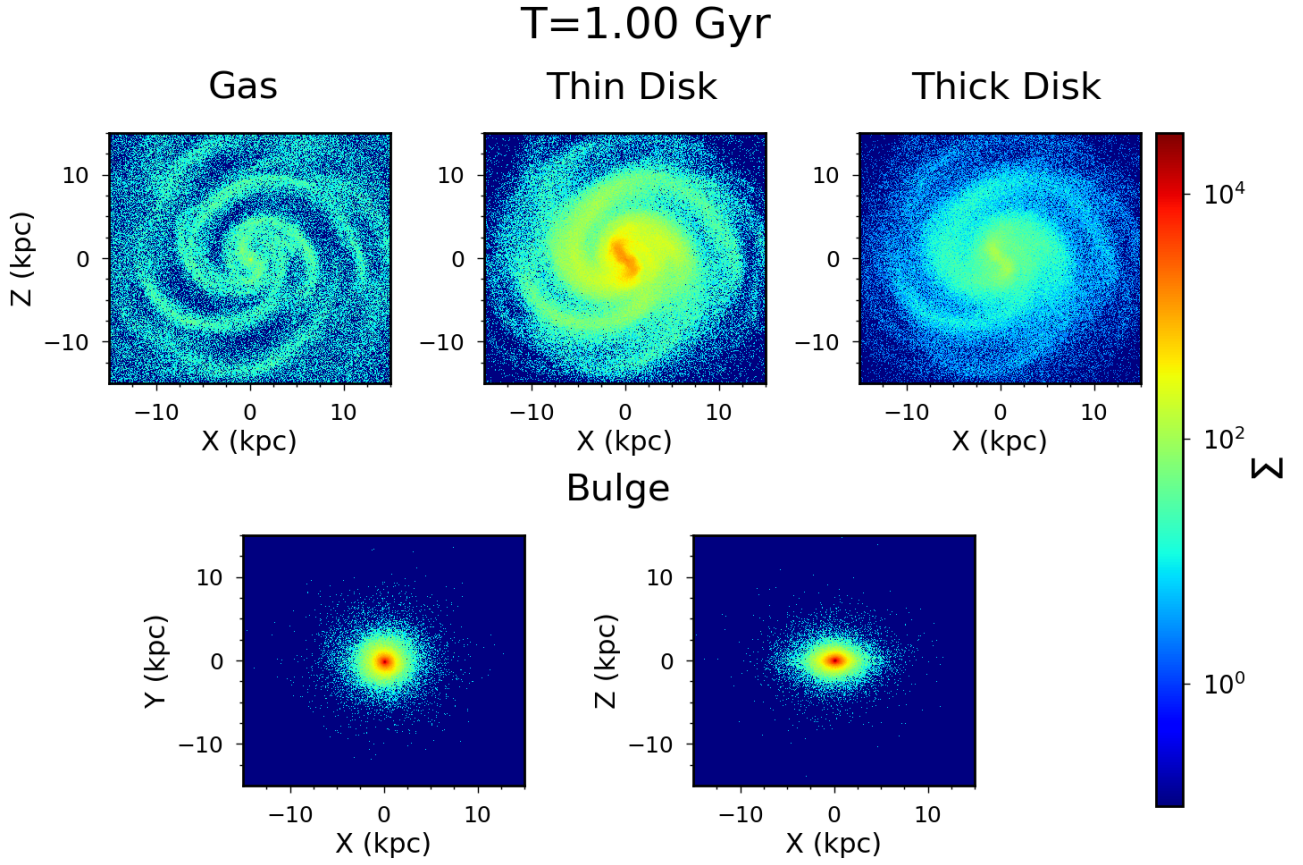


Figure 12. The $X - Y$ surface density for the gas disc, thin and thick discs, and the $X - Y$ and $X - Z$ surface density of the bulge. The surface density is in units of $M_{\odot} \text{pc}^{-2}$.

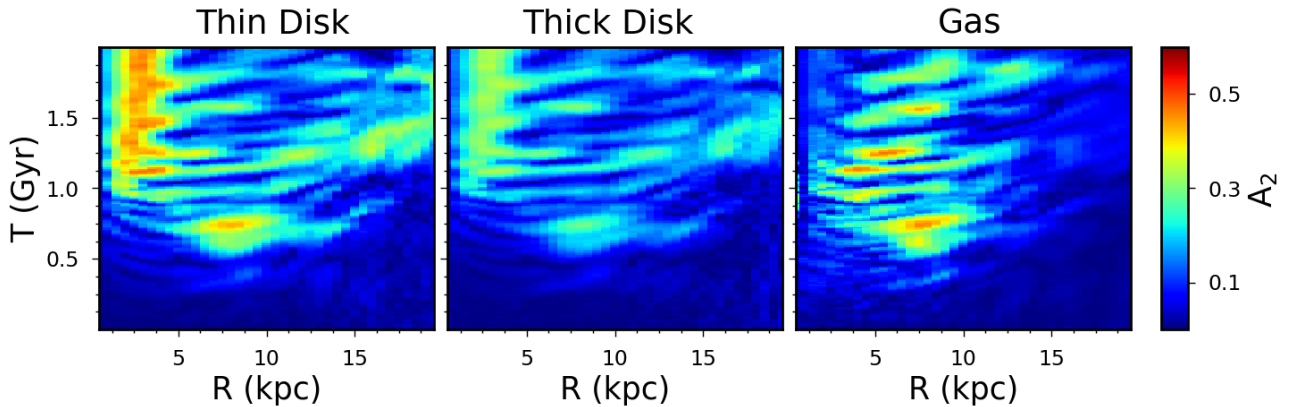


Figure 13. The A_2 moment as a function of radius and time for the thin, thick, and gas discs.

ICs that can be used to study the dynamics of observationally-motivated galaxy models. The inclusion of a gas disc opens up new and exciting possibilities that we are eager to explore in future work. Indeed, the models have already been used to study the rotation curves of barred spiral galaxies (Randriamampandry et al. 2018). Many stan-

dard algorithms for galaxy modelling fail for particular bar orientations. A suite of tailored ICs generated with GALACTICS allowed us to model galaxies of this type. The simulations shown in the present work suggest that dynamical simulations combined with observations might allow one to

constrain the models in a fashion not possible with mass models of the type considered in [McMillan \(2017\)](#).

CC's work is based upon research supported by the South African Research Chairs Initiative (SARChI) of the Department of Science and Technology (DST), the SKA SA and the National Research Foundation (NRF). ND's work is supported by a SARChI's South African SKA Fellowship. LMW is supported by the Natural Sciences and Engineering Research Council of Canada through Discovery Grants. The numerical simulations were performed at the Centre for High Performance Computing.

REFERENCES

- Athanassoula, E., 1983, in E. Athanassoula (ed.), *Internal Kinematics and Dynamics of Galaxies*, Dordrecht: D. Reidel Publishing Co., p. 243
- Athanassoula, E., Misiriotis, A., 2002, *MNRAS*, 330, 35
- Athanassoula, E., 2003, *MNRAS*, 341, 1179
- Athanassoula, E., Rodionov, S. A., Peschken, N., Lambert, J. C., 2016, *ApJ*, 821, 90
- Athanassoula, E., 2018, *IAU Symp.*, 334, 65
- Bekki, K., Tsujimoto, T., 2011, *MNRAS*, 416, L60
- Binney, J., 1987, in *The Galaxy*, ed. G. Gilmore & B. Carswell (Dordrecht: Reidel), 399
- Binney J., Tremaine S., 2008, *Galactic Dynamics: Second Edition*. Princeton Univ. Press, Princeton, NJ
- Bissantz, N., Gerhard, O., 2002, *MNRAS*, 330, 591
- Bottema, R., 1993, *A&A*, 275, 16
- Chequers, M. H., Widrow, L. M., 2017, *MNRAS*, 472, 2751
- Chequers, M. H., Widrow, L. M., & Darling, K. 2018, *MNRAS*, 480, 4244
- Debattista, V. P., Ness, M., Gonzalez, O. A., Freeman, K., Zoccali, M., Minniti D., 2017, *MNRAS*, 469, 1587
- Fujii, M. S., Bédorf, J., Baba, J., Portegies Zwart, S., 2019, *MNRAS*, 482, 1983
- Fragkoudi, F., Di Matteo, P., Haywood, M., Gómez, A., Combes, F., Katz, D., Semelin, B., 2017, *A&A*, 606, A47
- Fux, R., 1997, *A&A*, 327, 983
- Hernquist, L., 1993, *ApJS*, 86, 389
- Kazantzidis, S., Magorrian, J., Moore, B. 2004, *ApJ*, 601, 37
- Kuijken K., Dubinski J., 1995, *MNRAS*, 277, 1341
- Lokas, E. L., Ebrova, I., Pino, A. d., Semczuk, M., 2014, *MNRAS*, 445, L6
- McMillan, P. J., Dehnen, W., 2007, *MNRAS*, 378, 541
- McMillan, P. J., 2017, *MNRAS*, 465, 76
- Purcell, C. W., Bullock, J. S., Tollerud, E. J., Rocha, M., Chakrabarti, S., 2011, *Nature*, 477, 301
- Randriamampandry, T. H., Deg, N., Carignan, C., Widrow, L. 2018, *A&A*, 618, A106
- Rodionov, S. A., Sotnikova, N. Y., 2005, *Astron. Rep.*, 49, 470
- Rodionov, S. A., Athanassoula, E., Sotnikova, N. Y., 2009, *MNRAS*, 392, 904
- Rodionov, S. A., Athanassoula, E., 2011, *A&A*, 529, A98
- Schwarzschild, M., 1979, *ApJ*, 232, 236
- Sellwood, J. A., 1985, *MNRAS*, 217, 127
- Shu, F. H., 1969, *ApJ*, 158, 505
- Springel, V., 2005, *MNRAS*, 464, 1105
- Springel, V., Di Matteo, T., Hernquist, L., 2005, *MNRAS*, 361, 776
- Taranu, D. S., et al. 2017, *ApJ*, 850, 70
- Teyssier, R., 2002, *A&A*, 385, 337
- Vasiliev, E. 2019, *MNRAS*, 482, 1525
- Wang, H.-H., Klessen, R. S., Dullemond, C. P., van den Bosch, F. C., Fuchs, B., 2010, *MNRAS*, 407, 705
- Widrow, L. M., Dubinski, J., 2005, *ApJ*, 631, 838

Widrow, L. M., Pym, B., Dubinski, J., 2008, *ApJ*, 679, 1239

Yurin, D., Springel, V., 2014, *MNRAS*, 444, 62

This paper has been typeset from a $\text{\TeX}/\text{\LaTeX}$ file prepared by the author.